

Perturbation Method for Acoustic Multipole Logging in Transversely Isotropic Medium

Yongchun Gao^{1, a, *}, Xingang Guo², Jianwei Lu³

¹Department of Physics, College of Science, North China University of Science and Technology, Tangshan 063009, China

²School of Control Engineering, Northeastern University at Qinhuangdao, Qinghuangdao 066004, China

³Qingong College, North China University of Science and Technology, Tangshan 063009, China

^agaoyc1963@ncst.edu.cn

Abstract

A new and effective analytical perturbation method is presented for the multipole acoustic logging in a transversely isotropic medium (TIM) whose symmetric principal axis is parallel to the borehole axis although the exact solutions could be found. In this paper, the new perturbation method is adopted to simulate the full-waveforms in a borehole surrounded by a TIM for the first time. The TIM is regarded as a reference unperturbed isotropic state added to the perturbations, and three perturbation quantities about moduli deviated from the isotropic medium are introduced. By selecting a group of displacement potentials and a cylindrical coordinate system oriented along the borehole axis, the zero-, first-order and second-order perturbation solutions of the multipole acoustic field are derived for the weak transversely isotropic elastic solid which has its symmetric principal axis parallel to the borehole axis. The acoustic fields inside and outside the borehole excited by a multipole source are investigated. The full-waveforms in the borehole are numerically simulated by the perturbation method in the range of the second perturbation solutions. It is found that the full-waveforms inside the borehole excited by monopole, dipole sources and quadrupole source are similar to obtained by the exact solution.

Keywords

Perturbation, Transversely Isotropic Medium, reflection coefficient

1. Introduction

It has been found that wave propagation in an anisotropic medium has become a more active research topic. The interest of the study of the anisotropic formation is on the transversely isotropic medium (TIM) instead of others. This is mainly due to PTL (periodic thin-layer) and EDA (extensive-dilatancy anisotropy) models, which are important to the reservoir rocks and are all equivalent to the transversely isotropic formation in the hypothesis of the long wavelength. Along with the development of well logging technology to study acoustic wave propagation in anisotropic medium become more and more important for acoustics logging. If the medium outside the borehole is TIM, the wave field solution can be only solved in analytical form when the symmetric principal axis of TIM is parallel to the borehole axis. To study the wavefield characteristics in an important case when the symmetric principal axis of TIM is not parallel to the borehole axis, some approximation methods has been presented. Ellefsen, Sinha and Norris presented a perturbation method and examined the influence of weak elastic anisotropic on the tube wave speed^[1-5]. Their perturbation methods can only be applied to analyze for the guided waves. Zhang *et al.*^[6] conducted such method to study the guided waves in a borehole surrounded by a cubic crystal anisotropic medium. However, their perturbation methods cannot be used to investigate the characteristic of the full-wave as well as P and S waves. Zhang *et al.*^[7-9] presented another perturbation method that can treat the full-wave acoustic field for TIM with the principal axis perpendicular to the borehole axis. They obtained zero- and first- order

approximation solutions for the acoustic fields inside and outside the borehole. This method can be possibly used to analyze analytically the shear wave splitting in the borehole. However, they have not yet given the results of numerical simulation in detail.

In this Paper, we will give an extension perturbation analysis on the base of Zhang's method [7-9]. Not only the zero- and first- order but also the second- order approximation perturbation solutions are obtained for the first time when TIM's principal axis is parallel to the borehole axis. The acoustical fields inside and outside the borehole are numerically simulated by the perturbation method in the range of the second perturbation solutions. The acoustical fields are also compared and analyzed to that obtained by the exact solution. The objective of this paper is to prove the validity of the perturbation method by comparison to the exact solution and give a theoretical foundation for extending the perturbation analysis to complicated anisotropic acoustical logging.

2. Formulation

Consider a fluid-filled borehole surrounded by a transversely isotropic elastic solid whose symmetric principal axis is parallel to the borehole axis. The density and velocity of the fluid inside the borehole are ρ_f and V_f , respectively, and R is the radius of the borehole. We adopt a cylindrical coordinate system (r, θ, z) centered at the multipole source and oriented along the borehole axis, and define a Cartesian reference frame (x, y, z) whose z axis is parallel to the borehole axis.

In the Cartesian and coordinate system (x, y, z) , the displacement \mathbf{U} satisfies

$$\begin{aligned} (A-N)\frac{\partial^2 U_y}{\partial x \partial y} + (F+L)\frac{\partial^2 U_z}{\partial x \partial z} + N\frac{\partial^2 U_x}{\partial y^2} + L\frac{\partial^2 U_x}{\partial z^2} + A\frac{\partial^2 U_x}{\partial x^2} &= \rho \frac{\partial^2 U_x}{\partial t^2}, \\ A\frac{\partial^2 U_y}{\partial y^2} + L\frac{\partial^2 U_y}{\partial z^2} + N\frac{\partial^2 U_y}{\partial x^2} + (F+L)\frac{\partial^2 U_z}{\partial y \partial z} + (A-N)\frac{\partial^2 U_x}{\partial x \partial y} &= \rho \frac{\partial^2 U_y}{\partial t^2}, \\ (F+L)\frac{\partial^2 U_y}{\partial y \partial z} + L\frac{\partial^2 U_z}{\partial y^2} + C\frac{\partial^2 U_z}{\partial z^2} + L\frac{\partial^2 U_z}{\partial x^2} + (F+L)\frac{\partial^2 U_x}{\partial x \partial z} &= \rho \frac{\partial^2 U_z}{\partial t^2}. \end{aligned} \quad (1)$$

where A, C, F, L, N are five elastic constants (moduli), and ρ is the density.

Introduce three perturbation quantities $\varepsilon_1, \varepsilon_2$ and ε_3 by

$$\begin{aligned} \varepsilon_1 &= (F+2L-A)/L, \\ \varepsilon_2 &= (C-A)/L, \\ \varepsilon_3 &= (N-L)/L. \end{aligned} \quad (2)$$

when $\varepsilon_1, \varepsilon_2$ and ε_3 are equal to zero, the medium becomes to isotropy. It is easy to obtain by (1) and (2) that

$$(A-L)\nabla(\nabla \cdot \mathbf{U}) + L\nabla^2 \mathbf{U} - \rho \frac{\partial^2 \mathbf{U}}{\partial t^2} = \mathbf{G}, \quad (3)$$

where the components of the vector \mathbf{G} are

$$\begin{aligned} G_x &= L\varepsilon_3 \frac{\partial^2 U_y}{\partial x \partial y} - L\varepsilon_1 \frac{\partial^2 U_z}{\partial x \partial z} - L\varepsilon_3 \frac{\partial^2 U_x}{\partial y^2}, \\ G_y &= -L\varepsilon_3 \frac{\partial^2 U_y}{\partial x^2} - L\varepsilon_1 \frac{\partial^2 U_z}{\partial y \partial z} + L\varepsilon_3 \frac{\partial^2 U_x}{\partial x \partial y}, \\ G_z &= -L\varepsilon_1 \frac{\partial^2 U_y}{\partial y \partial z} - L\varepsilon_2 \frac{\partial^2 U_z}{\partial z^2} - L\varepsilon_1 \frac{\partial^2 U_x}{\partial x \partial z}. \end{aligned} \quad (4)$$

Expand the displacement

$$\begin{aligned}
 \mathbf{U} &= \mathbf{U}^{(0)} + \mathbf{U}^{(1)} + \mathbf{U}^{(2)} + \dots, \\
 \mathbf{U} &= \nabla\phi + \nabla \times (\chi \mathbf{e}_z) + \nabla \times \nabla \times (\psi \mathbf{e}_z), \\
 \phi &= \phi^{(0)} + \phi^{(1)} + \phi^{(2)} + \dots, \\
 \psi &= \psi^{(0)} + \psi^{(1)} + \psi^{(2)} + \dots, \\
 \chi &= \chi^{(0)} + \chi^{(1)} + \chi^{(2)} + \dots.
 \end{aligned}
 \tag{5}$$

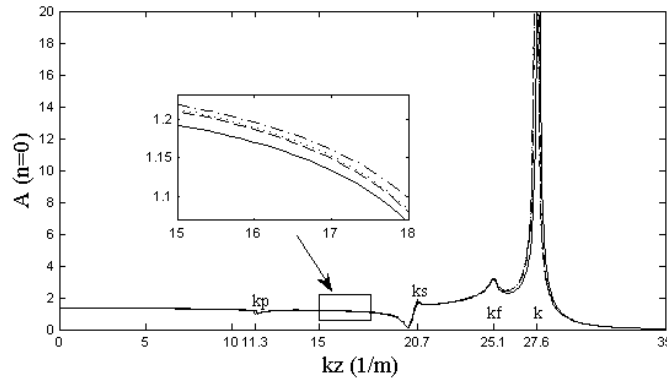


Fig.1. $n=0$, $f=6000\text{Hz}$, reflection coefficient A_0 , 1 solid line--isotropic, 2 dashed line--add first-order perturbation solutions, 3 dotted line--add second-order perturbation solutions, 4 dashed line--exact anisotropic(VTI) solutions.

Where ϕ , ψ , and χ are the displacement potentials of P, SV, and SH waves. The superscripts (0), (1), and (2) represent the zero-, first-, and second- order expanding quantities, respectively. Then, the zero-, first-, and second- order field equations can be written as

$$\begin{aligned}
 (A - L)\nabla(\nabla \cdot \mathbf{U}^{(0)}) + L\nabla^2\mathbf{U}^{(0)} - \rho \frac{\partial^2\mathbf{U}^{(0)}}{\partial t^2} &= 0 \\
 (A - L)\nabla(\nabla \cdot \mathbf{U}^{(1)}) + L\nabla^2\mathbf{U}^{(1)} - \rho \frac{\partial^2\mathbf{U}^{(1)}}{\partial t^2} &= \mathbf{G}^{(1)} \\
 (A - L)\nabla(\nabla \cdot \mathbf{U}^{(2)}) + L\nabla^2\mathbf{U}^{(2)} - \rho \frac{\partial^2\mathbf{U}^{(2)}}{\partial t^2} &= \mathbf{G}^{(2)}
 \end{aligned}
 \tag{6}$$

Where the components of $\mathbf{G}^{(1)}$ and $\mathbf{G}^{(2)}$ are given by Eq.(4) with the zero- and first- order displacement fields, respectively.

The first equation in Eq. (6) is just the field equation in isotropic medium. If the acoustic field is excited by an n th-order multipole source at $r=0$, the zero-order displacement potentials in the frequency wavenumber (ω, k_z) domain can be written as^[10-11]

$$\begin{aligned}
 \phi^{(0)} &= \alpha_1^{(0)} K_n(v_p r) \cos n(\theta - \theta_0), \\
 \psi^{(0)} &= \alpha_2^{(0)} K_n(v_s r) \cos n(\theta - \theta_0), \\
 \chi^{(0)} &= \alpha_3^{(0)} K_n(v_s r) \sin n(\theta - \theta_0).
 \end{aligned}
 \tag{7}$$

Where K_n is the second kind of n th-order modified Bessel function, $v_p = \sqrt{k_z^2 - k_p^2}$, $v_s = \sqrt{k_z^2 - k_s^2}$, $k_p^2 = \rho\omega^2 / A$, $k_s^2 = \rho\omega^2 / L$, and $\alpha_1^{(0)}$, $\alpha_2^{(0)}$, $\alpha_3^{(0)}$ are the weighting coefficients.

Putting the zero solution into the right side of the second equation of Eq.(6), a group of particular solutions, which satisfy the radiation condition at infinity, of the first-order perturbation is obtained by strict derivation.

$$\begin{aligned} \phi^{(1)} &= \frac{L}{A} \frac{k_z^2}{2v_p^2} \left[2\varepsilon_1 - (2\varepsilon_1 - \varepsilon_2) \frac{k_z^2}{k_p^2} \right] r \frac{\partial}{\partial r} \phi^{(0)} \\ &\quad + \frac{ik_z Lv_s^2}{A(k_p^2 - k_s^2)} \left[\varepsilon_1 - (2\varepsilon_1 - \varepsilon_2) \frac{k_z^2}{k_s^2} \right] \psi^{(0)}, \\ \psi^{(1)} &= \frac{ik_z}{k_s^2 - k_p^2} \left[\varepsilon_1 - (2\varepsilon_1 - \varepsilon_2) \frac{k_z^2}{k_p^2} \right] \phi^{(0)} + (2\varepsilon_1 - \varepsilon_2) \frac{k_z^2}{2k_s^2} r \frac{\partial}{\partial r} \psi^{(0)}, \\ \chi^{(1)} &= -\frac{\varepsilon_3}{2} r \frac{\partial}{\partial r} \chi^{(0)}. \end{aligned} \tag{8}$$

Similarly, Putting the first-order solution into the right side of the third equation of Eq.(6), a group of particular solutions about the second-order perturbation is

$$\begin{aligned} \phi^{(2)} &= \frac{k_z^2}{2v_p^2} \frac{L}{A} \left[2\varepsilon_1 + (\varepsilon_2 - 2\varepsilon_1) \frac{k_z^2}{k_p^2} \right] \left[\frac{L}{A} \frac{k_z^2}{2v_p^2} \left(2\varepsilon_1 - (2\varepsilon_1 - \varepsilon_2) \frac{k_z^2}{k_p^2} \right) r \frac{\partial}{\partial r} r \frac{\partial}{\partial r} \phi^{(0)} \right] \\ &\quad + \frac{k_z^2}{k_p^2 - k_s^2} \frac{L}{A} \left[2\varepsilon_1 + (\varepsilon_2 - 2\varepsilon_1) \frac{k_z^2}{k_s^2} \right] \left[\frac{ik_z Lv_s^2}{A(k_p^2 - k_s^2)} \left(\varepsilon_1 - (2\varepsilon_1 - \varepsilon_2) \frac{k_z^2}{k_s^2} \right) \psi^{(0)} \right] \\ &\quad + ik_z \frac{L}{2A} \left[\varepsilon_1 + (\varepsilon_2 - 2\varepsilon_1) \frac{k_z^2}{k_p^2} \right] \left[\frac{ik_z}{k_s^2 - k_p^2} \left(\varepsilon_1 - (2\varepsilon_1 - \varepsilon_2) \frac{k_z^2}{k_p^2} \right) r \frac{\partial}{\partial r} \phi^{(0)} \right] \\ &\quad + \frac{ik_z}{k_p^2 - k_s^2} \frac{Lv_s^2}{A} \left[\varepsilon_1 + (\varepsilon_2 - 2\varepsilon_1) \frac{k_z^2}{k_s^2} \right] \left[(2\varepsilon_1 - \varepsilon_2) \frac{k_z^2}{2k_s^2} r \frac{\partial}{\partial r} \psi^{(0)} \right], \\ \psi^{(2)} &= \frac{ik_z}{k_s^2 - k_p^2} \left[\varepsilon_1 + (\varepsilon_2 - 2\varepsilon_1) \frac{k_z^2}{k_p^2} \right] \left[\frac{L}{A} \frac{k_z^2}{2v_p^2} \left(2\varepsilon_1 - (2\varepsilon_1 - \varepsilon_2) \frac{k_z^2}{k_p^2} \right) r \frac{\partial}{\partial r} \phi^{(0)} \right] \\ &\quad + \frac{ik_z}{2v_s^2} \left[\varepsilon_1 + (\varepsilon_2 - 2\varepsilon_1) \frac{k_z^2}{k_s^2} \right] \left[\frac{ik_z Lv_s^2}{A(k_p^2 - k_s^2)} \left(\varepsilon_1 - (2\varepsilon_1 - \varepsilon_2) \frac{k_z^2}{k_s^2} \right) r \frac{\partial}{\partial r} \psi^{(0)} \right] \\ &\quad - (\varepsilon_2 - 2\varepsilon_1) \frac{k_z^2}{k_s^2 - k_p^2} \frac{v_p^2}{k_p^2} \left[\frac{ik_z}{k_s^2 - k_p^2} \left(\varepsilon_1 - (2\varepsilon_1 - \varepsilon_2) \frac{k_z^2}{k_p^2} \right) \phi^{(0)} \right] \\ &\quad - (\varepsilon_2 - 2\varepsilon_1) \frac{k_z^2}{2k_s^2} \left[(2\varepsilon_1 - \varepsilon_2) \frac{k_z^2}{2k_s^2} r \frac{\partial}{\partial r} r \frac{\partial}{\partial r} \psi^{(0)} \right], \\ \chi^{(2)} &= -\frac{\varepsilon_3}{2} \left[-\frac{\varepsilon_3}{2} r \frac{\partial}{\partial r} r \frac{\partial}{\partial r} \chi^{(0)} \right]. \end{aligned} \tag{9}$$

Therefore, the total displacement and stress fields can be represented in the range of the second-order perturbation by Eqs. (5), (7), (8), and (9).

The acoustical potential in the borehole for an n th multipole source can be written the same form as that in the isotropic medium [7,12]

$$\varphi_n^f = -\frac{1}{4\pi^2 n!} \left(\frac{vr_0}{2}\right)^n [\varepsilon_n K_n(vr) \cos n(\theta - \theta_0) + A_n I_n(vr) \cos n(\theta - \theta_0)]. \quad (10)$$

where $v = \sqrt{k_z^2 - \omega^2 / V_f^2}$ and V_f is the speed of the fluid inside the borehole, $\varepsilon_n = 2 - \delta_{n0}$ is Neumann's factor, r_0 is the multipole source separation, I_n is the first kind of the n th-order modified Bessel function, and A_n is the reflection coefficient which can be determined by the boundary conditions at borehole wall.

The boundary conditions at $r=R$ are [7, 10]

$$\begin{aligned} U_r^I &= U_r^{II}, \\ -P_f^I &= \tau_{rr}^{II}, \\ 0 &= \tau_{rz}^{II}, \\ 0 &= \tau_{r\theta}^{II}, \end{aligned} \quad (11)$$

where the superscripts I and II represent the media inside and outside the borehole. Substituting the fields inside and outside the borehole into Eqs. (11), yields a linear equation group about A_n , $\alpha_1^{(0)}$, $\alpha_2^{(0)}$, and $\alpha_3^{(0)}$. By this linear equation, we can calculate all unknown coefficients inside and outside the borehole. Then, it is easy to analyze the wavefield characteristics by numerical simulation. We will give the numerical results in the second-order perturbation analysis in the following.

3. Numerical simulation

In numerical simulation, the multipole source separation radius, the borehole radius, the acoustical velocity and density of the fluid inside the borehole are taken to be 0.01m, 0.1m, 1500m/s, and 1000kg/m³, respectively. The parameters of the two media are given in Table 1. The group 1 is for isotropic medium and is taken as the reference unperturbed states. The group 2 corresponds to the anisotropic medium, which is taken as the perturbation states added on the isotropic medium. The perturbation quantities ε_1 , ε_2 and ε_3 are all equal to 10%. The perturbation and analytic solutions will be shown in the range of the second approximation, by adding 10% perturbation on the reference unperturbed state.

Table1. Elastic constants of transversely isotropic material in unit 10¹⁰ N/m².

Note	A	L	N	C	F	ρ (kg/m ³)
1(isotropic)	2.7219664	0.8082256	0.8082256	2.7219664	1.1055152	2440
2(anisotropic)	2.7219664	0.8082256	0.8890482	2.80278896	1.1863378	2440

In numerical simulation, the displacement potentials (ϕ , ψ , and χ) inside the borehole and the reflection coefficient (A_n) outside borehole are studied, and the differences between the perturbation and analytic solutions are analyzed.

Figure 1 is relationship between the reflection coefficient (A_n) and different wave numbers (k_z) of monopole source ($n=0$) with the frequency 6000 Hz. We use the solid line represents the isotropic medium result, the dash line for the perturbation result with first-order, the dot line for the perturbation result with second-order, the dot-dash line for anisotropic medium (TIM). For the isotropic medium, as the parameters of group 1 in Table 1, the wave-number of press wave, shear wave, fluid wave and guided wave are 11.3, 20.7, 25.1, 27.6, respectively. The velocity of guided wave (Stoneley wave) is about 1362.5 m/s. As we can see from Figure 1 that when $kz=27.6$, the curve of reflection coefficient corresponds the maximum point. So it is temporarily proved the results are correct. The parameters

of anisotropic medium define that it is a weakly anisotropic medium, which means the differences of velocities in different direction are similar. So as we can see from Figure 1 that four different curves are hardly separated. We magnify the curves in the range of $kz=(15,18)$ in order to solve the problem. Then we can see clearly that the curve of isotropic medium is on the bottom, as the perturbation's order increases, the corresponding curve is more close to the curve of the anisotropic medium. The perturbation method is valid.

Figure 2 is on the condition of dipole source ($n=1$). The line style setting is the same with Figure 1. The guided wave velocity of dipole source (flexural wave) is about 1607.2 m/s, this corresponds the wave number point $kz=19.5$. The reflection coefficient curve of isotropic medium also achieves its maximum point. We cut the line nearby the maximum point because its value is so large that we cannot observe the condition of low wavenumber area. Also, for observe the curves clearly, we magnify the curves of the range $kz=(8,10)$. Then we can identify each curve easily. The curve of isotropic medium is on the bottom, and the curves are more close to the curve of anisotropic medium while the perturbation's order increases.

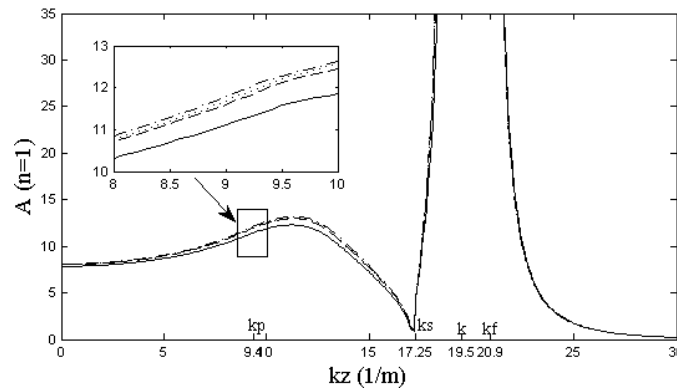


Fig.2. $n=1$, $f=5000\text{Hz}$, reflection coefficient $A1$, 1 solid line--isotropic, 2 dashed line--add first-order perturbation solutions, 3 dotted line--add second-order perturbation solutions, 4 dashed line--exact anisotropic(VTI) solutions.

Last, we research the results of quasi-pole source in order to further confirmation the perturbation method is valid and stable. The results are shown in Figure 3. We magnify the curves in the range $kz=(12,14)$. It is clearly that the curve is very close to the anisotropic medium when the first-order perturbation is added. And the curve of adding second-order perturbation is more close to the anisotropic medium curve than that of adding first-order perturbation.

So we can infer that the perturbation method is stable and valid to simulate anisotropic medium. The precision of the results becomes accurate while the number of perturbation order increases.

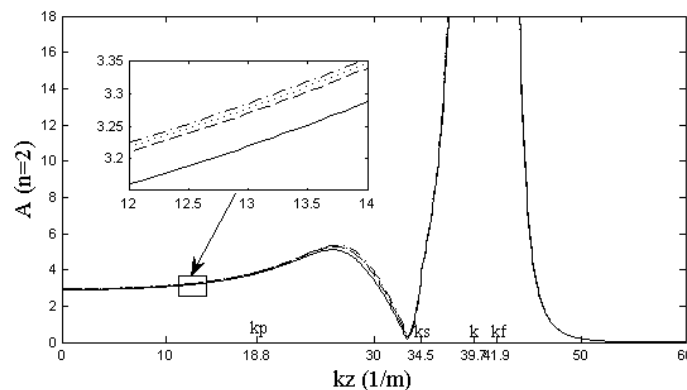


Fig.3. $n=2$, $f=10000\text{Hz}$, reflection coefficient $A2$, 1 solid line--isotropic, 2 dashed line--add first-order perturbation solutions, 3 dotted line--add second-order perturbation solutions, 4 dashed line--exact anisotropic(VTI) solutions.

4. Conclusions

In conclusion, the multipole reflection coefficient in a fluid-filled borehole surrounded by a TIM are studied by the perturbation method. For cross reference, the analytic results of reflection coefficient in an isotropic and an anisotropic media are also given. The perturbation analyses are carried out by introducing the perturbation quantity on the reference state. By numerical simulation, the reflection coefficient of multipole source are investigated. The numerical results show that the perturbation method is a feasible method by comparison to the analytic solutions which can be applied to the complicated anisotropic medium in acoustic logging.

References

- [1] K. J. Ellefsen, C. H. Cheng, and M. N. Toksöz, *J. Geophys. Res.* 96 537 (1991).
- [2] B. K. Sinha, *Ferroelectrics*. 41 61 (1982).
- [3] A. N. Norris, B. K. Sinha, and S. Kostek, *Geophys. J. Int.* 118 439 (1994).
- [4] B. K. Sinha, A. N. Norris, and S. K. Chang, *Geophysics*. 59 1037 (1994).
- [5] A. N. Norris, B. K. Sinha, *J. Acoust. Soc. Am.* 98 1147 (1995).
- [6] L. Zhang, B. X. Zhang, and K. X. Wang, *Chin. Phys. Lett.* 24 3179 (2007).
- [7] B. X. Zhang, Ph.D. Thesis (Jilin University) (1994).
- [8] B. X. Zhang, and K. X. Wang, *J. Acoust. Soc. Am.* 99 2674 (1996).
- [9] B. X. Zhang, and K. X. Wang, *Chinese J. Geophys.* 43 707 (2000).
- [10] A. L. Kurkjian, and S. K. Cheng, *Geophysics*. 51 148 (1986).
- [11] D. P. Schmitt, C. H. Cheng, and M. N. Toksöz, *SPWLA 28th Annual Logging Symposium* (1987).
- [12] D. P. Schmitt, *J. Acoust. Soc. Am.* 86 2397 (1989).